

Characterization of Endothelial Cells Associated with Cerebral Arteriovenous Malformation

This article was published in the following Dove Press journal:
Neuropsychiatric Disease and Treatment

Yu-Chen Jia^{1,*}
Jia-Yue Fu^{2,*}
Ping Huang³
Zhan-Pu Zhang³
Bo Chao³
Jie Bai³

¹Inner Mongolia Key Laboratory of Molecular Biology, School of Basic Medical Sciences, Inner Mongolia Medical University, Hohhot, People's Republic of China; ²Inner Mongolia Medical University, Hohhot, People's Republic of China; ³Department of Neurosurgery, Affiliated Hospital, Inner Mongolia Medical University, Hohhot, People's Republic of China

*These authors contributed equally to this work

Introduction: Cerebral arteriovenous malformation (cAVM) is a disease characterized by the angiogenesis and remodeling of veins. However, whether vascular endothelial cells (ECs) exhibit morphological and functional changes during cAVM remains unclear. This study aimed to investigate the role of ECs in the pathogenesis of cAVM.

Methods: Rat model of cAVM was established by anastomosing the common carotid artery with the external jugular vein. The digital subtraction angiography (DSA), HE, Masson and immunohistochemical staining were performed to evaluate the model. ECs were isolated from AVM rat model or control rats, and characterized by MTT, cell scratch, and tube formation assays. The secretion of vascular endothelial growth factor (VEGF) was detected by ELISA.

Results: AVM rat model showed typical pathological characteristics of cAVM. In addition, the proliferation, migration and tube formation abilities of ECs of arterIALIZED vein (AV-ECs) were significantly better than those of ECs of normal vein (NV-ECs). Moreover, the levels of secreted VEGF were significantly higher in AV-ECs than in NV-ECs.

Conclusion: AV-ECs isolated from AVM rat model showed increased proliferation, migration and angiogenesis and may be potential target for the treatment of cAVM.

Keywords: cerebral arteriovenous malformation, endothelial cell, angiogenesis, VEGF

Introduction

Cerebral arteriovenous malformation (cAVM) involves the vessels which are abnormally formed, and becomes a key factor of seizure and intracranial hemorrhage.¹ During cAVM active angiogenesis and vascular remodeling develop, indicating that cAVM is not a congenital cerebrovascular disease.^{2,3} As a biomechanical stimulus, wall shear stress is responsible for vascular remodeling during cAVM, in which endothelial cells (ECs) play an important role.⁴ The understanding of the pathogenesis of cAVM is limited by the lack of appropriate animal models.

In a previous study, cranial external jugular vein (EJV) and common carotid artery (CCA) were anastomosed to create a rat model to analyze histopathological, hemodynamic and angiographic characteristics of cAVM.⁵ Additional study showed morphological similarities between the model and human AVM vessels such as heterogeneously thickened walls, splitting of elastic lamina, thickened endothelial layers, endothelial cushions, lack of tight junction, loss of endothelial continuity, endothelial-subendothelial adherent junction, and lumenally directed filopodia. These findings suggest that increased flow in cAVM results in vascular changes, and support the use of the model to reveal the mechanism of cAVM in human.⁶

Correspondence: Jie Bai
Department of Neurosurgery, Affiliated Hospital, Inner Mongolia Medical University, No. 1 Tongdao North Road, Hohhot City, Inner Mongolia 010000, People's Republic of China
Tel +86-471-6351352
Fax +86-471-6351184
Email baijie0611@126.com

Therefore, in this study we used this rat model of cAVM to isolate and characterize ECs. Our aim is to investigate the role of ECs in the pathogenesis of cAVM, especially in the processes of angiogenesis and vascular remodeling.

Materials and Methods

Animals

All experiments were approved by the Animal Care and Use Committee of the Inner Mongolia Medical University in accordance with the guidelines of the National Institutes of Health guide for the care and use of Laboratory animals. Sprague-Dawley male rats (7 weeks old, 180 ± 13 g) were provided by Inner Mongolia Medical University and AVM model was established by anastomosing common carotid artery with external jugular vein as described previously.⁵ Three rats were used in AVM model group and three rats were used in normal control group. The digital subtraction angiography (DSA) was used to confirm that the anastomotic stoma was unobstructed in 42 days after the fistula. The angiography was performed under conditions of strict sterility, the hearts of the rats were exposed and 3 mL contrast agent was injected from left ventricle, and then X-ray was used to observe blood flow. The rats were euthanized via intraperitoneal injection of barbiturate.

Histological and Immunohistochemical Staining

The arterialized vein (AV) was isolated from one rat in AVM model group while the normal vein (NV) was isolated from one rat in control group. The tissues were fixed in 4% paraformaldehyde for 12 h, embedded in paraffin, cut into sections (10 μ m thin), and three sections in each group were stained with hematoxylin and eosin (H&E) and Masson. Other three sections in each group were stained with CD31 antibody (Abcam, ab119339) and alpha smooth muscle actin (SMA) antibody (Boiss, bs-10196R) using immunohistochemical kit (MXB, 40443a).

Transmission Electron Microscopy (TEM)

Each rat in model and control groups were anesthetized and perfused with a solution of 2% sucrose, 2% glutaraldehyde, 2% lanthanum nitrate and 0.1 M sodium cacodylate. The vein tissues were then fixed in perfusion solution, embedded in epoxy resin, and cut into ultrathin sections (90 nm). Three sections from each group were stained with

uranyl acetate and lead citrate, and examined under TEM (HT-7700; Hitachi, Japan).

Primary Culture of ECs

The vessels from AV of each rat in AVM model group and control group were cut longitudinally, the vascular explants were cut into about 2 mm² tissue block and put into 6-well plates. Then the explants were cultured in EGM-2 media (LONZA, USA) supplemented with 5% fetal bovine serum (FBS), hydrocortisone 0.1 mL/L, hFGF-B 1 mL/L, VEGF 0.25 mL/L, R3-IGF-1, 0.25 mL/L, ASCORBIC ACID, 0.25 mL/L, hEGF 0.25 mL/L, GA-1000 0.25 mL/L, HEPARIN 0.25 mL/L) at 37°C in a humidified incubator with 5% CO₂. Adherent cells formed a single layer in 15 days. The culture medium was changed every 3 days. When adherent cells reached 80% confluence, they were digested, suspended and subcultured.

Immunofluorescence Staining

Cells were seeded into 12-well plates with cover glass at a concentration of 2×10^5 cells/well, and incubated overnight at 37°C. Then the cells were washed twice with phosphate-buffered saline (PBS), fixed for 10 min in 4% paraformaldehyde, and treated with 0.2% Triton X-100 to permeabilize the cell membranes. The cells were blocked with 3% albumin bovine fraction V (Coolaber, CA1381-5G) and then incubated with CD31 antibody (1:150, Abcam, ab119339) and VE-Cadherin antibody (1:100, SANTA, sc-9989) overnight at 4°C. The next day, the cells were incubated with Anti-Von Willebrand Factor (FITC) (1:75, Abcam, ab8822) and Goat anti mouse IgG (1:100, Proteintech, SA00013-3), and treated with DAPI (Beyotime, C1005) to stain the nuclei. The cells were observed under a confocal microscope (LSM900, ZEISS, Germany). All experiments were performed in triplicates.

MTT Assay

Cells were seeded into 96-well plates at a density of 1×10^4 cells/well. The cells were cultured at 37°C for 1d, 3d, 5d. 20 μ L MTT solution (5 mg/mL; Sigma-Aldrich) was then added to each well. Following incubation for 4 h at 37°C, the medium was discarded, and 150 μ L DMSO (Sangon Biotech) was added to each well. The plates were agitated for 15 min, and the optical density values at 490 nm were measured in triplicate using an ELISA monitor (Bio-Rad). All experiments were performed in triplicates.

Cell Scratch Assay

The cells were plated at 2×10^5 /well in 6-well plates. After the cells had reached 70–80% confluence, a scratch was made across the cell layer using a pipette tip. Then the floating cells and cell debris were washed away by PBS for three times. The cells were cultured in serum-free EGM-2 medium at 37°C. The distance of cells movement was evaluated and photographed under a microscope at 0 h, 18 h and 24 h. The rate of scratch wound healing was calculated by using image J software. All experiments were performed in triplicates.

Tube Formation Assay

Tube formation assay was conducted using Matrigel Basement Membrane Matrix (Corning, Cat: 356,234,

USA). 96-well plates were pre-coated with matrigel and then cells were seeded at a concentration of 10^4 cells/well, and incubated at 37°C in 5% CO₂, and tube formation was photographed under a microscope at 6 h, 12 h, and 24 h and analyzed by image J software. All experiments were performed in triplicates.

Enzyme-Linked Immunosorbent Assay

Enzyme-Linked immunosorbent assay (ELISA) was performed using ELISA kit for vascular endothelial growth factor (VEGF) (Cloud-Clone Corp, Cat: SEA143Ra, China) following the manufacturer's instructions. The optical density values at 450 nm were measured in triplicate using an ELISA monitor (Bio-Rad). All experiments were performed in triplicates.

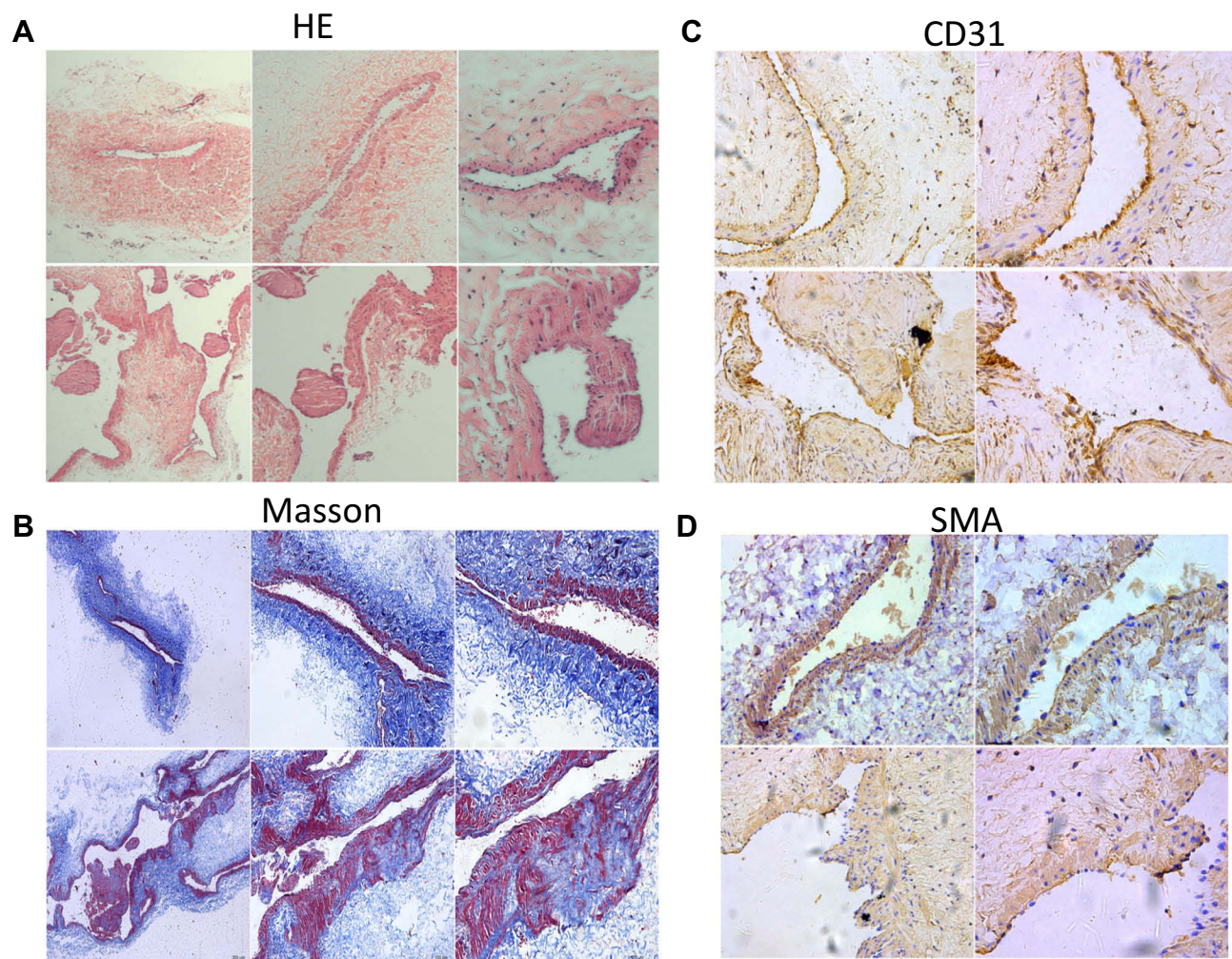


Figure 1 Gross morphology of the normal external jugular vein (EJV) and the arterIALIZED EJV showed by HE staining (A) and Masson staining (B). We observed vascular dilatation, thin wall, discontinuous and irregular intima, incomplete elastic layer, dysplasia of the medial membrane, disordered smooth muscle arrangement, increased collagen fibers and smooth muscle protruding into the lumen of AV. The discontinuity of AV's endothelial cells was shown based on CD31 staining (C), and the changes of AV's smooth muscle such as hyperplasia, disordered and protruding into the lumen were shown based on SMA staining (D) (original magnification, A, X10 (upper panel), X20 (lower panel), B X4, X10, X20 (from left to right), C, D X20, X40 (from left to right)).

Statistical Analysis

Statistical analysis was performed using SPSS statistical package (version 22.0). All experimental data were presented as Mean \pm SD from at least three independent experiments. *T*-test and Mann–Whitney Test were used, and the results were considered statistically significant if *P* value was less than 0.05.

Results

Pathological Characteristics of the Vein in AVM Model

Histologic examination and Masson staining of the AV showed the appearance of vascular dilatation, thin wall, discontinuous intima, incomplete elastic layer, dysplasia of the medial membrane, disordered smooth muscle arrangement, increased collagen fibers, irregular intima and smooth muscle protruding into the lumen (Figure 1A and B). CD31 staining showed discontinuity of endothelial cells of AV (Figure 1C). SMA staining showed that

smooth muscle of AV had hyperplasia, were disordered and protruded into the lumen (Figure 1D).

Electron micrographs of endothelial cells from the vein of control rats (NV-ECs) showed normal ultrastructure (Figure 2A). In contrast, electron micrographs of endothelial cells from arterIALIZED vein (AV-ECs) in AVM rat model showed ultrastructure damages, including mitochondria and endoplasmic reticulum swelling, disappeared mitochondrial crista and lysosome formation (Figure 2B–F). These results revealed similar pathological characteristics between cAVM and AVM rat model.

Higher Proliferation Rate of AV-ECs

The AV-ECs and NV-ECs were isolated from AVM rats and control rats and cultured. They showed characteristics of vascular ECs with slender protuberances on cell surface (Figure 3A), and positive expression of CD31, vWF and VE-Cadherin (Figure 3B–D). However, MTT assay showed that the proliferation rate of AV-ECs was significantly higher than that of NV-ECs (Figure 3E).

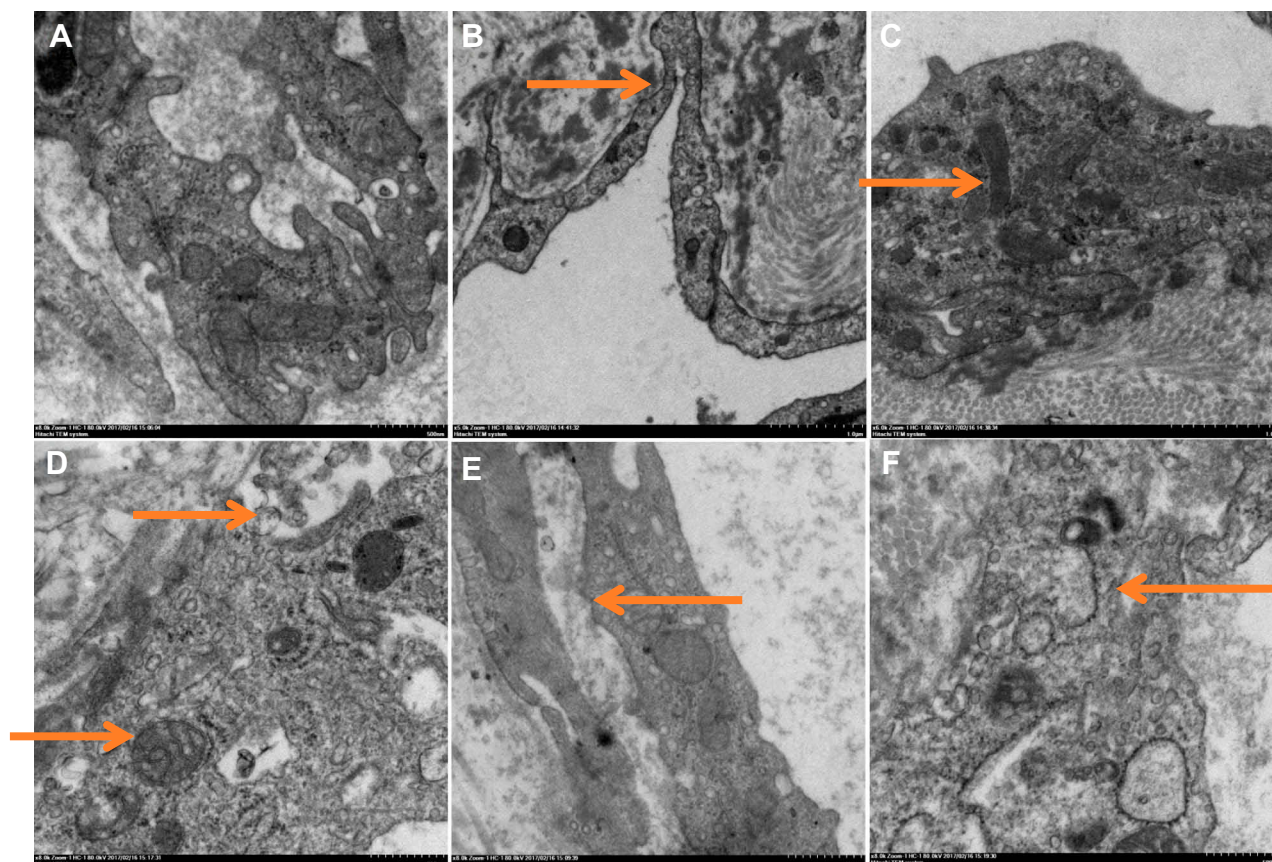


Figure 2 Electron micrographs of endothelial cells of normal veins (A) and arterIALIZED veins in AVM rat model (B–E). (A) Normal organelles. (B) Occluding junction of vascular endothelial cells (indicated by arrow). (C) WP body (indicated by arrow). (D) Mitochondria swelling and lysosome formation (indicated by arrows). (E) Mitochondrial crista disappeared (indicated by arrow). (F) Endoplasmic reticulum swelling (indicated by arrow).

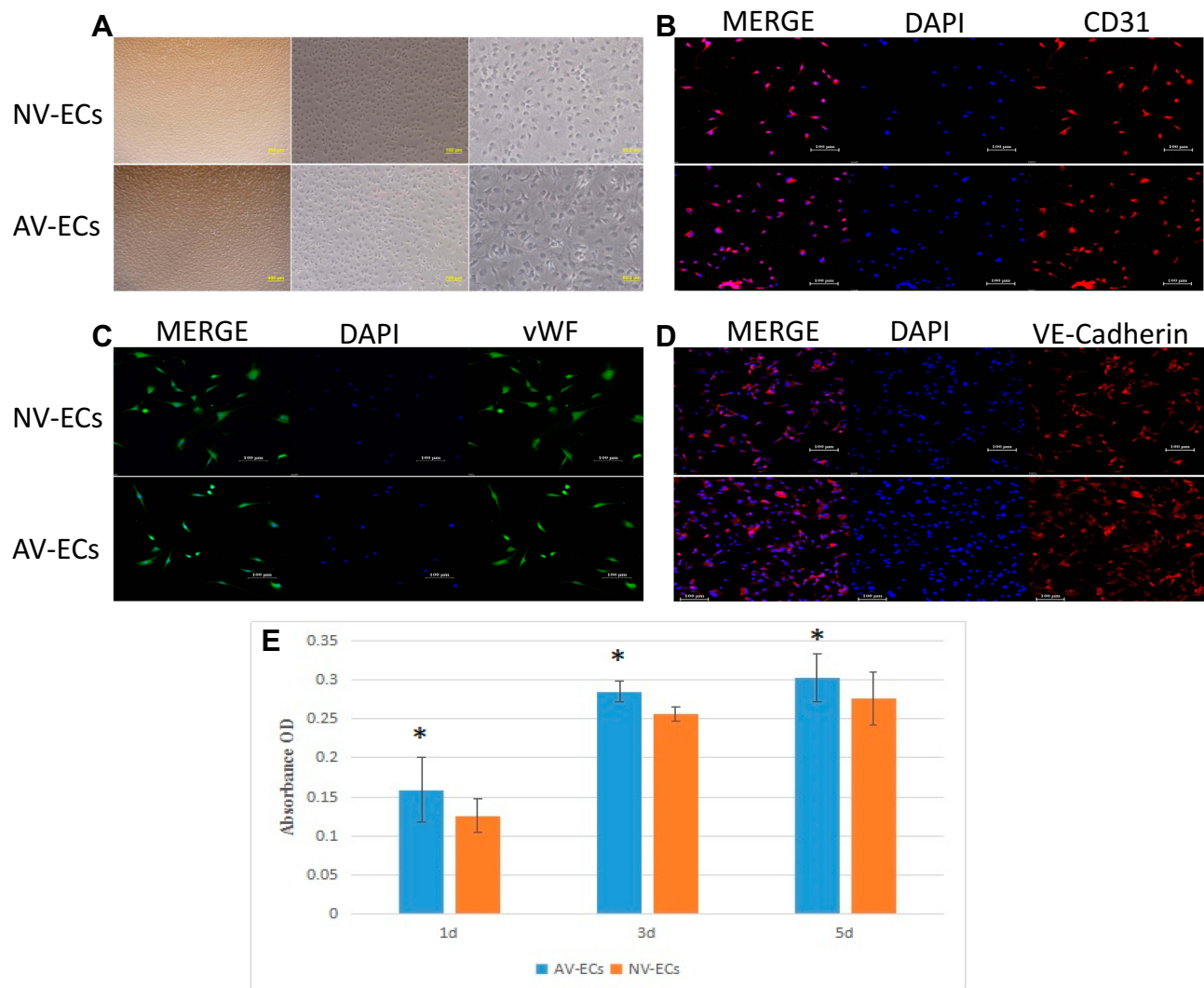


Figure 3 Proliferation of AV-ECs and NV-ECs. Morphology of AV-ECs and NV-ECs (A, magnification 4X, 10X, 20X). Immunostaining of CD31 (B), vWF (C) and VE-Cadherin (D) (magnification 20X). The nuclei were stained as blue by DAPI. MTT assay of the proliferation of AV-ECs and NV-ECs at 1d, 3d and 5d (E). Data are mean \pm SD (n=3). *P<0.05 between AV-ECs and NV-ECs.

Higher Migration Ability of AV-ECs

To compare migration ability of AV-ECs and NV-ECs, we performed cell scratch assay (Figure 4A). Quantitative analysis showed that the migration of AV-ECs was significantly higher than that of NV-ECs (Figure 4B).

Stronger Tube Formation of AV-ECs

To compare angiogenesis of AV-ECs and NV-ECs, we performed tube formation assay (Figure 5A). Quantitative analysis showed that the tube length of AV-ECs was significantly higher than that of NV-ECs (Figure 5B). Furthermore, ELISA analysis of the concentration of VEGF in cell culture supernatant showed that the concentration of VEGF secreted by AV-ECs was significantly higher than that of NV-ECs after culture for 3 d, 6 d and 9 d (Figure 5C).

Discussion

cAVM is a cerebrovascular disease mainly treated by microsurgery currently, but there are some treatment-related risks.^{7,8} cAVM has been shown to occasionally regrow after resection and radiotherapy.^{9,10} Histological analysis showed that the levels of angiogenic factors were higher in cAVM than in the normal vessels.^{11–13} The difficulty of primary culture of ECs in human cAVM and lack of applicable animal models are two main obstacles for the development of effective treatment for cAVM.

Previously, a AVM model was established based on the anastomosing of common carotid artery with external jugular vein and the model has already been used for the investigations of cAVM.⁶ In this study we used this AVM model and observed endothelial cushions, multiple layers

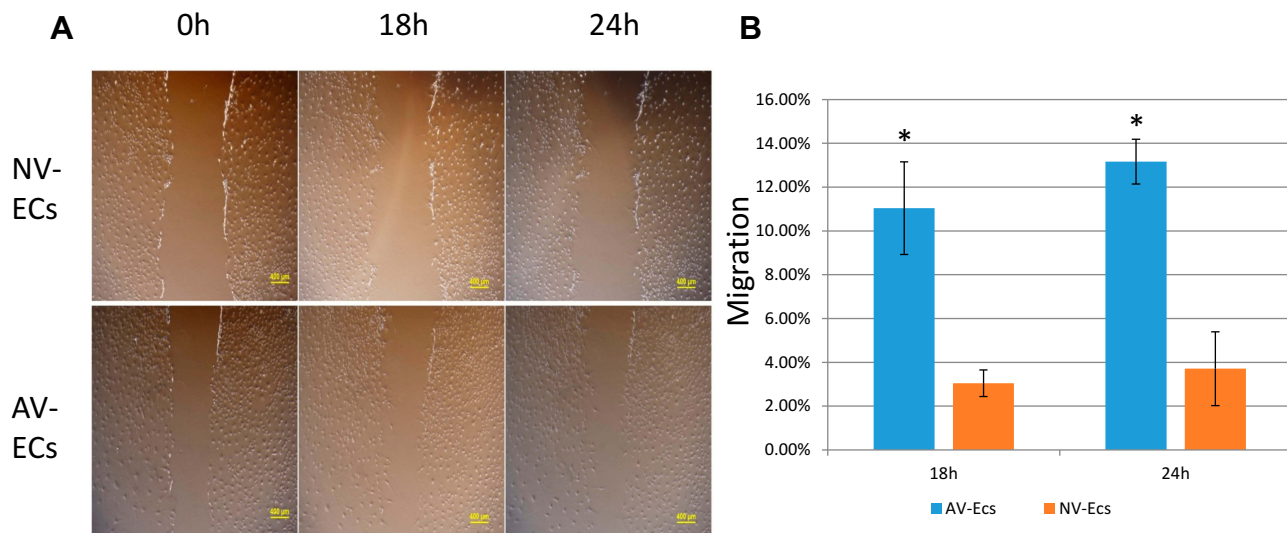


Figure 4 Migration of AV-ECs and NV-ECs. Cell scratch assay of the gap in AV-ECs and NV-ECs at 0 h, 18 h and 24 h (A). The migration rate was measured by using Image J (B). Data are mean ± SD (n=3). *P<0.05 between AV-ECs and NV-ECs.

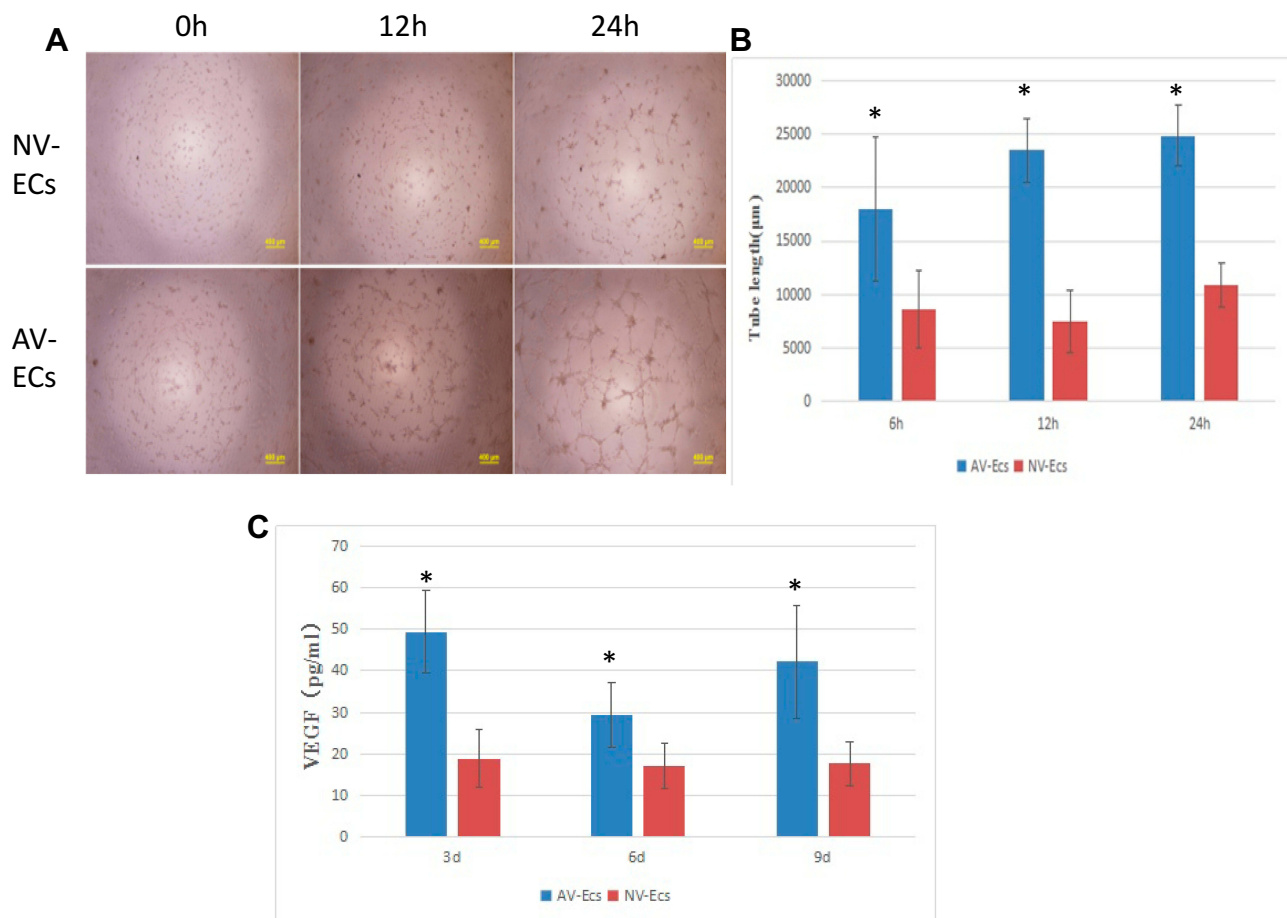


Figure 5 Angiogenesis of AV-ECs and NV-ECs. Tube formation assay of AV-ECs and NV-ECs at 6 h, 12 h and 24 h (A). The tube length was measured by using Image J (B). VEGF concentration was detected by ELISA (C). Data are mean ± SD (n=3). *P<0.05 between AV-ECs and NV-ECs.

of endothelial cells, splitting of the elastic lamina, more prominent smooth muscle cells and high capillary density. It was proposed that cerebral venous hypertension resulted in a pro-angiogenic state and may trigger cAVM development.^{14,15} The endothelial and smooth muscle cells are activated by high shear stress which promotes the release of angiogenic factors and other cytokines essential for vascular remodeling.^{16–18}

However, the role of ECs in the pathogenesis of cAVM is still not clear. Therefore, in this study we isolated and cultured AV-ECs from AVM model rats, and then compared their biological characteristics with ECs from control rats. We found that AV-ECs had stronger proliferation, migration and tube formation ability. Indeed, a previous study reported that the proliferative activity of vascular endothelial cells in cAVM is situated between normal vessels and tumor vessels.² The first phase of angiogenesis involves the migration and proliferation of ECs, which can result in the growth of cAVM after resection. Vascular endothelial growth factor (VEGF) is a key mediator of angiogenesis because it can increase the proliferation of ECs.^{2,19} In addition, the permeability of blood brain barrier (BBB) is increased by VEGF and other angiogenic factors. This could make vascular walls more likely to rupture.²⁰ In this study, we found higher level of VEGF secretion in AV-ECs. These results suggest that increased secretion of VEGF may promote the proliferation, migration and angiogenesis of ECs in the development of cAVM. However, further studies are needed to elucidate the mechanism by which increased flow in cAVM induces the production and secretion of VEGF.

In conclusion, increased proliferation, migration and angiogenesis of vascular ECs isolated from AVM rat model indicated that biological characteristics of these cells have changed. Further characterization of these ECs will help understand the pathogenesis of cAVM.

Funding

This study was supported by grants from The National Natural Science Fund, China (No. gizr15204), the Inner Mongolian Natural Science Fund (No. 2015MS(LH)0802) and Kejibaiwan Project of Inner Mongolia Medical University (No. YKD2013KJBW009).

Disclosure

Yu-Chen Jia and Jia-Yue Fu are co-first authors for this study. The authors declare no competing interests.

References

- Alkadhhi H, Kollias SS, Crelier GR, Golay X, Hepp-Reymond MC, Valavanis A. Plasticity of the human motor cortex in patients with arteriovenous malformations: a functional MR imaging study. *Am J Neuroradiol.* 2000;21(8):1423–1433.
- Hashimoto T, Mesa-Tejada R, Quick CM, et al. Evidence of increased endothelial cell turnover in brain arteriovenous malformations. *Neurosurgery.* 2001;49(1):124–131. doi:10.1097/00006123-200107000-00019
- Kader A, Goodrich JT, Sonstein WJ, Stein BM, Carmel PW, Michelsen WJ. Recurrent cerebral arteriovenous malformations after negative postoperative angiograms. *J Neurosurg.* 1996;85(1):14–18. doi:10.3171/jns.1996.85.1.0014
- Alaraj A, Shakur SF, Amin-Hanjani S, et al. Changes in wall shear stress of cerebral arteriovenous malformation feeder arteries after embolization and surgery. *Stroke.* 2015;46(5):1216–1220. doi:10.1161/STROKEAHA.115.008836
- Yassari R, Sayama T, Jahromi BS, Aihara Y, Stoodley M, Macdonald RL. Angiographic, hemodynamic and histological characterization of an arteriovenous fistula in rats. *Acta Neurochir (Wien).* 2004;146(5):495–504. doi:10.1007/s00701-004-0248-x
- Tu J, Karunanayaka A, Windsor A, Stoodley MA. Comparison of an animal model of arteriovenous malformation with human arteriovenous malformation. *J Clin Neurosci.* 2010;17(1):96–102. doi:10.1016/j.jocn.2009.02.044
- Spetzler RF, Martin NA. A proposed grading system for arteriovenous malformations. *J Neurosurg.* 1986;65(4):476–483. doi:10.3171/jns.1986.65.4.0476
- Han PP, Ponce FA, Spetzler RF. Intention-to-treat analysis of Spetzler-Martin Grades IV and V arteriovenous malformations: natural history and treatment paradigm. *J Neurosurg.* 2003;98(1):3–7. doi:10.3171/jns.2003.98.1.0003
- Klimo P Jr, Rao G, Brockmeyer D. Pediatric arteriovenous malformations: a 15-year experience with an emphasis on residual and recurrent lesions. *Childs Nerv Syst.* 2007;23(1):31–37. doi:10.1007/s00381-006-0245-x
- Lindqvist M, Karlsson B, Guo WY, Kihlstrom L, Lippitz B, Yamamoto M. Angiographic long-term follow-up data for arteriovenous malformations previously proven to be obliterated after gamma knife radiosurgery. *Neurosurgery.* 2000;46(4):803–808. doi:10.1097/00006123-200004000-00006
- Bai J, Wang YJ, Liu L, Zhao YL. Ephrin B2 and EphB4 selectively mark arterial and venous vessels in cerebral arteriovenous malformation. *J Int Med Res.* 2014;42(2):405–415. doi:10.1177/0300060513478091
- Hashimoto T, Wu Y, Lawton MT, Yang GY, Barbaro NM, Young WL. Coexpression of angiogenic factors in brain arteriovenous malformations. *Neurosurgery.* 2005;56(5):1058–1065.
- Guo Y, Saunders T, Su H, et al. Silent intralesional microhemorrhage as a risk factor for brain arteriovenous malformation rupture. *Stroke.* 2012;43(5):1240–1246. doi:10.1161/STROKEAHA.111.647263
- Chen L, Gao Z, Liu B, Lv Y, An M, Febg J. Circumferential variation in mechanical characteristics of porcine descending aorta. *Biocell.* 2018;42(1):25–34. doi:10.32604/biocell.2018.06114
- Gao P, YQ Z, Ling F, et al. Nonischemic cerebral venous hypertension promotes a pro-angiogenic stage through HIF-1 downstream genes and leukocyte-derived MMP-9. *J Cereb Blood Flow Metab.* 2009;29(8):1482–1490. doi:10.1038/jcbfm.2009.67
- Hofer IE, van Royen N, Rectenwald JE, et al. Arteriogenesis proceeds via ICAM-1/Mac-1-mediated mechanisms. *Circ Res.* 2004;94(9):1179–1185. doi:10.1161/01.RES.0000126922.18222.F0
- Tzima E, Del Pozo MA, Shattil SJ, Chien S, Schwartz MA. Activation of integrins in endothelial cells by fluid shear stress mediates Rho-dependent cytoskeletal alignment. *EMBO J.* 2001;20(17):4639–4647. doi:10.1093/emboj/20.17.4639

18. Jiang W, Wang M. New insights into the immunomodulatory role of exosomes in cardiovascular disease. *Rev Cardiovasc Med.* 2019;20(3):153–160.
19. Jin Y, Muhl L, Burmakin M, et al. Endoglin prevents vascular malformation by regulating flow-induced cell migration and specification through VEGFR2 signalling. *Nat Cell Biol.* 2017;19(6):639–652. doi:10.1038/ncb3534
20. Ha Y, Kim TS, Yoon DH, Cho YE, Huh SG, Lee KC. Reinduced expression of developmental proteins (nestin, small heat shock protein) in and around cerebral arteriovenous malformations. *Clin Neuropathol.* 2003;22(5):252–261.

Neuropsychiatric Disease and Treatment

Dovepress

Publish your work in this journal

Neuropsychiatric Disease and Treatment is an international, peer-reviewed journal of clinical therapeutics and pharmacology focusing on concise rapid reporting of clinical or pre-clinical studies on a range of neuropsychiatric and neurological disorders. This journal is indexed on PubMed Central, the 'PsycINFO' database and CAS, and

is the official journal of The International Neuropsychiatric Association (INA). The manuscript management system is completely online and includes a very quick and fair peer-review system, which is all easy to use. Visit <http://www.dovepress.com/testimonials.php> to read real quotes from published authors.

Submit your manuscript here: <https://www.dovepress.com/neuropsychiatric-disease-and-treatment-journal>